Research Square

Preprints are preliminary reports that have not undergone peer review.
They should not be considered conclusive, used to inform clinical practice,
or referenced by the media as validated information.

Volumetric Analysis of Cerebellar Lobules in Spinocerebellar Ataxia 27B (SCA27B)

Aziz Benbachir
McGill University
Thiago JR Rezende
University of Campinas (UNICAMP)
Peiyuan Huang
McGill University
Shihan Chen
University of Alberta
Elisabetta Indelicato
Medical University of Innsbruck
Sylvia Boesch
Medical University of Innsbruck
Jonathan de Winter
University of Antwerp
Mathilde Renaud
CHRU Nancy
Guillemette Clement
CHRU Nancy
Pablo Iruzubieta
McGill University
David Pellerin
McGill University
Bernard Brais
McGill University
Marcondes C. França
University of Campinas (UNICAMP)
Roberta La Piana
roberta.lapiana@mcgill.ca

McGill University

Short Report

Keywords: Spinocerebellar Ataxias, Magnetic Resonance Imaging, Late onset cerebellar ataxias, SCA27B, Cerebellar Atrophy

Posted Date: August 10th, 2026

DOI: https://doi.org/10.21203/rs.3.rs-10193603/v1

License: This work is licensed under a Creative Commons Attribution 4.0 International License. Read Full License

Additional Declarations: No competing interests reported.

Abstract

Background

Spinocerebellar ataxia 27B (SCA27B) is an autosomal dominant, late-onset cerebellar ataxia caused by an intronic *FGF14* GAA•TTC repeat expansion and frequently associated with cerebellar atrophy. In this study, we aimed to quantitatively determine whether the cerebellar atrophy in SCA27B is predominantly localized to some sub-cerebellar regions and can be detected on clinical MR studies.

Methods

We analyzed 3D and/or sagittal T1-weighted MR images from 13 subjects with SCA27B (median age: 67 years, IQR: 9 years, 2 females; median GAA size 383) and 52 age- and sex-matched controls. Cerebellar segmentation was performed using the DeepCERES pipeline. For each region of interest, we calculated mean volume, standard deviation, and relative volume differences between groups. Analysis of covariance (ANCOVA) was used to test the effect of disease status on the volumes while adjusting for age and sex.

Results

The volume was significantly reduced in all regions of interest (at least − 10%) when compared to controls, except the whole white matter, lobules I–II and IX. The greatest relative volume difference was seen in lobules IV (-25%), VI (-18%), and X (-18%). Lobules IV and X, the grey matter and the whole cerebellum showed the greatest effect of disease status.

Conclusions

SCA27B is associated with diffuse cerebellar atrophy with relatively important involvement of lobules IV and X. Automated segmentation tools such as DeepCERES enable reliable volumetric characterization from clinical MRI and may support future comparative studies of SCA27B and other forms of late-onset ataxias.

Introduction

Spinocerebellar ataxia 27B (SCA27B) is a dominantly inherited, slowly progressive, late-onset cerebellar ataxia caused by a GAA•TTC (≥ 250) repeat expansion in intron 1 of the *Fibroblast Growth Factor 14* (FGF14) gene.[1–3] Patients typically present initially with episodic symptoms — most often gait ataxia and oculomotor abnormalities such as downbeat nystagmus — and eventually become permanently ataxic.[3, 4] Reported MRI findings in SCA27B include cerebellar atrophy in 38–97% of patients, predominantly involving the vermis [1, 2, 5–8] and abnormal T2-weighted hyperintense signal along the

superior cerebellar peduncles in 60–68% of patients [9, 10]. Since cerebellar function is topographically organized and specific diseases can affect specific cerebellar structures [11–13], it is important to characterize more precisely the pattern of cerebellar involvement in SCA27B. Importantly, identifying a defined pattern of cerebellar atrophy can guide genetic testing, assist in cases with unclear diagnosis, and overall accelerate the diagnostic process. Therefore, the aim of this study was to determine whether the atrophy observed in patients with SCA27B affects predominantly some sub-cerebellar regions and can be detected on clinical MR studies.

Methods

Participants

From the brain MRI studies of subjects with a molecularly confirmed diagnosis of SCA27B (i.e. evidence of GAA•TTC repeat expansion ≥ 250)[14] performed in the clinical setting and available to our team, we included those with available 3D or sagittal T1-weighted sequences containing at least 30 slices (n = 15), as per technical requirement of the DeepCERES pipeline, and then excluded those with failed segmentation defined as gross misclassification of regions by the segmentation algorithm or no output from the segmentation pipeline (n = 2). In the end, our analysis comprised 13 clinically acquired MRI studies from SCA27B patients (median age = 67, range = 58–76, 2 females) from 4 sites of recruitment (Montreal, Innsbruck, Antwerp and Nancy). Given the retrospective nature of the study, the severity of the ataxic symptoms or scale for assessment and rating of ataxia (SARA) scores at the time of MRI were not available.

We also included MR T1-weighted image datasets from age- and sex-matched healthy controls obtained from the Alzheimer's Disease Neuroimaging Initiative (n = 39) [15] and collaborators (n = 13), for a total of 52 controls, thus with a ratio of 4:1 healthy controls/patients.

Segmentation

Cerebella were segmented using the DeepCERES pipeline[16]. Example segmentations for patients and controls are provided in **Fig. 1**. Since we aimed to assess whether the atrophy is predominantly localized to specific lobules and subcerebellar regions, we considered the volumes of the following regions in percent of intracranial volume (%ICV) as computed by DeepCERES[16, 17]: Cerebellum, White Matter, Grey Matter, Lobules I-II, Lobule III, Lobule IV, Lobule V, Lobule VI, Crus I, Crus II, Lobule VIIB, Lobule VIIIA, Lobule VIIIB, Lobule IX, and Lobule X.

Data Analysis

For each region, we computed the mean and standard deviation of its volume in the SCA27B patient and control groups. We then computed the relative volume difference between patients and controls by using the following formula:

$$Relative\ difference = \frac{Mean\ volume\ in\ patients - Mean\ volume\ in\ controls}{Mean\ volume\ in\ controls} \cdot 100\ \%$$

Statistical significance of volume differences between SCA27B patients and controls was assessed using ANCOVA for each region with covariates Disease status, Age, and Sex. P values were corrected for multiple comparisons using the Benjamini-Hochberg procedure. All analyses were done in R. In addition to calculating the relative volume difference, we computed the Cohen's d coefficient for each region to obtain a measure of effect size of disease status (patients vs controls) on region volume differences. We considered Cohen's values below 0.2 as having small, 0.5 moderate, 0.8 large, and > 1.2 very large effect size of disease state.[18]

Results

The mean volume and standard deviations for each region of interest in subjects with SCA27B and controls are shown in Table 1. Except for the white matter, lobules I-II, and lobule IX, we observed a statistically significant reduction in the volumes of all other cerebellar regions of interest. Figure 2 illustrates the boxplots for each region of interest.

Figure 3 shows the relative volume differences between subjects with SCA27B and controls. Among all the regions showing statistically significant differences (Table 1), we documented a relative volume reduction of at least − 10% in subjects with SCA27B as compared to controls, with the whole cerebellum being 11% smaller. The regions with the greatest statistically significant relative volume difference were lobules IV (-25%), VI (-19%), and X (-18%).

Regarding the effect of disease status on each region of interest volume, all regions showed at least a moderate effect size. The regions with the greatest effect of disease status – all classified as very large effect size - were lobule IV (1.8), lobule X (1.5), as well as the grey matter (1.9) and whole cerebellum (1.6). Cohen's d values for all regions are shown in Fig. 4.

Discussion

This is the first study to quantitatively measure the cerebellar and sub-cerebellar volumes in clinical scans of SCA27B patients using an openly available, user-friendly segmentation tool not requiring specialized imaging analytical skills. As expected from previous qualitative studies, [1, 2, 5, 7, 8] we found that the cerebellum is significantly smaller in subjects with SCA27B than in controls, by at least − 10% of the relative volume in almost all examined regions and with a peak of -25% volume reduction in lobule IV. The fact that the white matter was one of the few regions with no statistically significant volume difference suggests that the cortical involvement drives the cerebellar volume reduction in SCA27B. In support of this suggestion, the grey matter showed the largest effect of disease status among all the examined structures. It should be noted, though, that the DeepCERES pipeline does not segment the deep cerebellar nuclei and instead counts their volume as white matter.

While we documented a relatively widespread pattern of cerebellar atrophy in SCA27B, lobules IV and X showed the largest effect of disease status between lobules of controls and subjects with SCA27B and the biggest relative volume difference (together with lobule VI). Of note, we also found important volume reduction in lobules I-II of subjects with SCA27B compared to controls, but with no statistically significant difference and small effect size of disease status. These findings could be due to the limitations resulting from segmenting such a small structure.

The availability of accurate, fast, and openly accessible cerebellar segmentation algorithms, such as DeepCERES has proven to be useful to quantify cerebellar atrophy using clinically available MR data. Importantly, DeepCERES has the advantage of being user-friendly, requiring no specialized neuroimaging expertise and no software installation. Therefore, the approach here reported facilitates the reproducibility of our results in cohorts and contexts where advanced imaging facilities and expertise are missing. Our study suggests the potential clinical utility of quantitative imaging assessments in routine radiological practice. Such an addition could be valuable for radiologists during clinical interpretation and reporting, particularly in improving the objectivity and sensitivity of imaging-based evaluations. Specifically, imaging measurements like those here described can be used in the clinical setting for quantifying cerebellar atrophy and supporting genetic testing results, especially when considering multiple cerebellar diseases with overlapping phenotypes. Previous studies have reported a particular decrease in the cerebellar grey matter and superior cerebellar vermis in SCA6,[19, 20] and lobules X and Crus II volumes in SCA3.[21, 22] In SCA2, the largest volumetric decrease occurs in lobules I-II, IV, and VI.[23]

Our study has several limitations. The small sample size restricts statistical power, and the retrospective clinically heterogeneous MR data may have introduced measurement variability. Therefore, our findings and their significance remain to be confirmed with future dedicated prospective studies. Additionally, we computed the volumes using predefined regions of interest. In future studies and larger cohorts, it will be interesting to conduct an unbiased analysis, for example using voxel-based morphometry, to detect patterns in a more data-driven way. Future work should also examine whether disease duration and severity at the time of MRI, and GAA •TTC repeat expansion size affect the patterns of cerebellar and sub-cerebellar atrophy in SCA27B.

In conclusion, SCA27B is associated with diffuse cerebellar atrophy with relatively important involvement of lobules IV and X. Automated cerebellar segmentation tools such as DeepCERES enable reliable volumetric measurements on clinical MRI and are potential tools for clinicians to quantify cerebellar atrophy and orient the differential diagnosis.

Declarations

Funding

RLP has received a Research Scholar Junior 1 and Junior 2 award from the Fonds de Recherche du Québec en Santé (FRQS), and research funds from the Canadian Institutes of Health Research (grant 506913), Ataxia Canada, the Spastic Paraplegia Foundation and the ARSACS Foundation. EI and SB are members of the European Reference Network for Rare Neurological Diseases (ERN-RND)—Project ID No 739510. DP holds a Fellowship award from the Canadian Institutes of Health Research

Competing Interests

The authors report no competing interests related to this work.

Ethics Approval

This study was performed in line with the principles of the Declaration of Helsinki. Approval was granted by the Research Ethics Board of the McGill University Health Center on June 12, 2025.

Consent to participate

Informed consent was obtained from all individual participants included in the study.

Author Contribution

Conceptualization and Study Design: Roberta La Piana; Data Collection: Elisabetta Indelicato, Sylvia Boesch, Jonathan de Winter, Mathilde Renaud, Guillemette Clement, Pablo Iruzubieta, David Pellerin, Bernard Brais, Thiago JR Rezende, Marcondes Franca; Data analysis: Aziz Benbachir, Shihan Chen, Peiyuan Huang; Writing - original draft preparation: Aziz Benbachir; Figures preparation: Aziz Benbachir; Writing - review and editing: all authors; Funding acquisition: Bernard Brais, Roberta La Piana; Supervision: Roberta La Piana.

Acknowledgement

RLP has received a Research Scholar Junior 1 and Junior 2 award from the Fonds de Recherche du Québec en Santé (FRQS), and research funds from the Canadian Institutes of Health Research (grant 506913), Ataxia Canada, the Spastic Paraplegia Foundation and the ARSACS Foundation. EI and SB are members of the European Reference Network for Rare Neurological Diseases (ERN-RND)—Project ID No 739510. DP holds a Fellowship award from the Canadian Institutes of Health Research

Data Availability

All the aggregated data supporting the findings of this study are available within the paper. The raw data are available upon request and with the permission from the authors.

References

1. Rafehi H, Read J, Szmulewicz DJ, Davies KC, Snell P, Fearnley LG, Scott L, Thomsen M, Gillies G, Pope K, et al. An intronic GAA repeat expansion in FGF14 causes the autosomal-dominant adult-onset ataxia SCA50/ATX-FGF14. Am J Hum Genet. 2023;110(1):105–19.
2. Pellerin D, Danzi MC, Wilke C, Renaud M, Fazal S, Dicaire MJ, Scriba CK, Ashton C, Yanick C, Beijer D, et al. Deep Intronic FGF14 GAA Repeat Expansion in Late-Onset Cerebellar Ataxia. N Engl J Med. 2023;388(2):128–41.
3. Clément G, Puisieux S, Pellerin D, Brais B, Bonnet C, Renaud M. Spinocerebellar ataxia 27B (SCA27B), a frequent late-onset cerebellar ataxia. Rev Neurol (Paris). 2024;180(5):410–6.
4. Pellerin D, Danzi M, Renaud M, Houlden H, Synofzik M, Zuchner S, Brais B. GAA-FGF14-Related Ataxia. In: *GeneReviews(®).* edn. Edited by Adam MP, Feldman J, Mirzaa GM, Pagon RA, Wallace SE, Amemiya A. Seattle (WA): University of Washington, Seattle Copyright © 1993–2025, University of Washington, Seattle. GeneReviews is a registered trademark of the University of Washington, Seattle. All rights reserved.; 1993.
5. Abou Chaar W, Eranki AN, Stevens HA, Watson SL, Wong DY, Avila VS, Delfeld M, Gary AJ, Tawde S, Triebold M, et al. Clinical, Radiological and Pathological Features of a Large American Cohort of Spinocerebellar Ataxia (SCA27B). Ann Neurol. 2024;96(6):1092–103.
6. Chen S, Ashton C, Sakalla R, Clement G, Planel S, Bonnet C, Lamont P, Kulanthaivelu K, Nalini A, Houlden H et al. Neuroradiological findings in GAA-FGF14 ataxia (SCA27B): more than cerebellar atrophy. *medRxiv* 2024.
7. Novis LE, Frezatti RS, Pellerin D, Tomaselli PJ, Alavi S, Della Coleta MV, Spitz M, Dicaire MJ, Iruzubieta P, Pedroso JL, et al. Frequency of GAA-FGF14 Ataxia in a Large Cohort of Brazilian Patients With Unsolved Adult-Onset Cerebellar Ataxia. Neurol Genet. 2023;9(5):e200094.
8. Iruzubieta P, Pellerin D, Bergareche A, Albajar I, Mondragón E, Vinagre A, Fernández-Torrón R, Moreno F, Equiza J, Campo-Caballero D, et al. Frequency and phenotypic spectrum of spinocerebellar ataxia 27B and other genetic ataxias in a Spanish cohort of late-onset cerebellar ataxia. Eur J Neurol. 2023;30(12):3828–33.
9. Chen S, Ashton C, Sakalla R, Clement G, Planel S, Bonnet C, Lamont PJ, Kulanthaivelu K, Nalini A, Houlden H, et al. Involvement of the Superior Cerebellar Peduncles in GAA-FGF14 Ataxia. Neurol Genet. 2025;11(2):e200253.
10. van Prooije TH, Pennings M, Maas R, de Vries J, Verschuuren-Bemelmans C, Odekerken V, Darweesh SKL, Huisman M, Oosterloo M, Buijink A et al. Clinical, Genetic, and Imaging Characteristics of SCA27B: Insights from a Large Dutch Cohort. Mov Disord 2026.
11. Eichler L, Bellenberg B, Hahn HK, Köster O, Schöls L, Lukas C. Quantitative assessment of brain stem and cerebellar atrophy in spinocerebellar ataxia types 3 and 6: impact on clinical status. AJNR Am J Neuroradiol. 2011;32(5):890–7.

12. Stefanescu MR, Dohnalek M, Maderwald S, Thürling M, Minnerop M, Beck A, Schlamann M, Diedrichsen J, Ladd ME, Timmann D. Structural and functional MRI abnormalities of cerebellar cortex and nuclei in SCA3, SCA6 and Friedreich's ataxia. Brain. 2015;138(Pt 5):1182–97.
13. Bang OY, Lee PH, Kim SY, Kim HJ, Huh K. Pontine atrophy precedes cerebellar degeneration in spinocerebellar ataxia 7: MRI-based volumetric analysis. J Neurol Neurosurg Psychiatry. 2004;75(10):1452–6.
14. Bonnet C, Pellerin D, Roth V, Clément G, Wandzel M, Lambert L, Frismand S, Douarinou M, Grosset A, Bekkour I, et al. Optimized testing strategy for the diagnosis of GAA-FGF14 ataxia/spinocerebellar ataxia 27B. Sci Rep. 2023;13(1):9737.
15. Petersen RC, Aisen PS, Beckett LA, Donohue MC, Gamst AC, Harvey DJ, Jack CR Jr., Jagust WJ, Shaw LM, Toga AW, et al. Alzheimer's Disease Neuroimaging Initiative (ADNI): clinical characterization. Neurology. 2010;74(3):201–9.
16. Morell-Ortega S, Ruiz-Perez M, Gadea M, Vivo-Hernando R, Rubio G, Aparici F, Iglesia-Vaya M, Catheline G, Mansencal B, Coupé P, et al. DeepCERES: A deep learning method for cerebellar lobule segmentation using ultra-high resolution multimodal MRI. NeuroImage. 2025;308:121063.
17. Manjón JV, Romero JE, Vivo-Hernando R, Rubio-Navarro G, De la Iglesia-Vaya M, Aparici-Robles F, Coupé P. Deep ICE: A deep learning approach for MRI intracranial cavity extraction. arXiv preprint arXiv:200105720 2020.
18. Schmitz-Hübsch T, Fimmers R, Rakowicz M, Rola R, Zdzienicka E, Fancellu R, Mariotti C, Linnemann C, Schöls L, Timmann D, et al. Responsiveness of different rating instruments in spinocerebellar ataxia patients. Neurology. 2010;74(8):678–84.
19. Butteriss D, Chinnery P, Birchall D. Radiological characterization of spinocerebellar ataxia type 6. Br J Radiol. 2005;78(932):694–6.
20. Lukas C, Schöls L, Bellenberg B, Rüb U, Przuntek H, Schmid G, Köster O, Suchan B. Dissociation of grey and white matter reduction in spinocerebellar ataxia type 3 and 6: a voxel-based morphometry study. Neurosci Lett. 2006;408(3):230–5.
21. Faber J, Schaprian T, Berkan K, Reetz K, França MC Jr., de Rezende TJR, Hong J, Liao W, van de Warrenburg B, van Gaalen J, et al. Regional Brain and Spinal Cord Volume Loss in Spinocerebellar Ataxia Type 3. Mov Disord. 2021;36(10):2273–81.
22. Piccinin CC, Rezende TJR, de Paiva JLR, Moysés PC, Martinez ARM, Cendes F, França MC Jr.. A 5-Year Longitudinal Clinical and Magnetic Resonance Imaging Study in Spinocerebellar Ataxia Type 3. Mov Disord. 2020;35(9):1679–84.
23. Nigri A, Sarro L, Mongelli A, Pinardi C, Porcu L, Castaldo A, Ferraro S, Grisoli M, Bruzzone MG, Gellera C, et al. Progression of Cerebellar Atrophy in Spinocerebellar Ataxia Type 2 Gene Carriers: A Longitudinal MRI Study in Preclinical and Early Disease Stages. Front Neurol. 2020;11:616419.

Table

Table 1. Comparison of observed volumes (normalized to intracranial volume) in SCA27B Patients vs Controls for all regions of interest. p values are adjusted for false discovery rate. Volumes are in percent of intracranial volume. *Legend*: SD, standard deviation; CI, confidence interval; SE, standard error.

	Mean (SD) Controls	**Mean (SD) Patients**	**β (95% CI)**	**SE**	**t**	**P value**
Cerebellum (%)	8.379 (0.571)	7.457 (0.540)	-0.937 (-1.261, -0.613)	0.162	-5.78	**<0.001**
White.Matter (%)	2.891 (0.159)	2.796 (0.212)	-0.099 (-0.204, 0.006)	0.053	-1.88	0.124
Grey.Matter (%)	5.488 (0.437)	4.662 (0.394)	-0.838 (-1.078, -0.599)	0.120	-7.00	**<0.001**
Lobules.I.II(%)	0.005 (0.002)	0.004 (0.002)	-0.001 (-0.002, 0.000)	0.001	-1.50	0.183
Lobule.III (%)	0.056 (0.011)	0.047 (0.010)	-0.009 (-0.016, -0.003)	0.003	-2.88	**0.015**
Lobule.IV (%)	0.195 (0.027)	0.146 (0.026)	-0.050 (-0.066, -0.034)	0.008	-6.19	**<0.001**
Lobule.V (%)	0.356 (0.046)	0.298 (0.043)	-0.059 (-0.086, -0.032)	0.014	-4.31	**<0.001**
Lobule.VI (%)	0.862 (0.135)	0.707 (0.149)	-0.157 (-0.234, -0.080)	0.038	-4.09	**<0.001**
Crus.I (%)	1.226 (0.160)	1.041 (0.185)	-0.187 (-0.286, -0.088)	0.049	-3.78	**<0.001**
Crus.II (%)	0.835 (0.102)	0.731 (0.072)	-0.105 (-0.166, -0.044)	0.031	-3.43	**0.003**
Lobule.VIIB (%)	0.518 (0.064)	0.450 (0.056)	-0.069 (-0.108, -0.030)	0.019	-3.58	**0.003**
Lobule.VIIIA (%)	0.607 (0.064)	0.526 (0.065)	-0.083 (-0.123, -0.043)	0.020	-4.17	**<0.001**
Lobule.VIIIB (%)	0.406 (0.049)	0.340 (0.053)	-0.068 (-0.098, -0.039)	0.015	-4.61	**<0.001**
Lobule.IX (%)	0.345 (0.065)	0.310 (0.054)	-0.036 (-0.074, 0.002)	0.019	-1.91	0.146
Lobule.X	0.077 (0.009)	0.063 (0.010)	-0.014 (-0.020, -0.008)	0.003	-4.94	**<0.001**

Figures

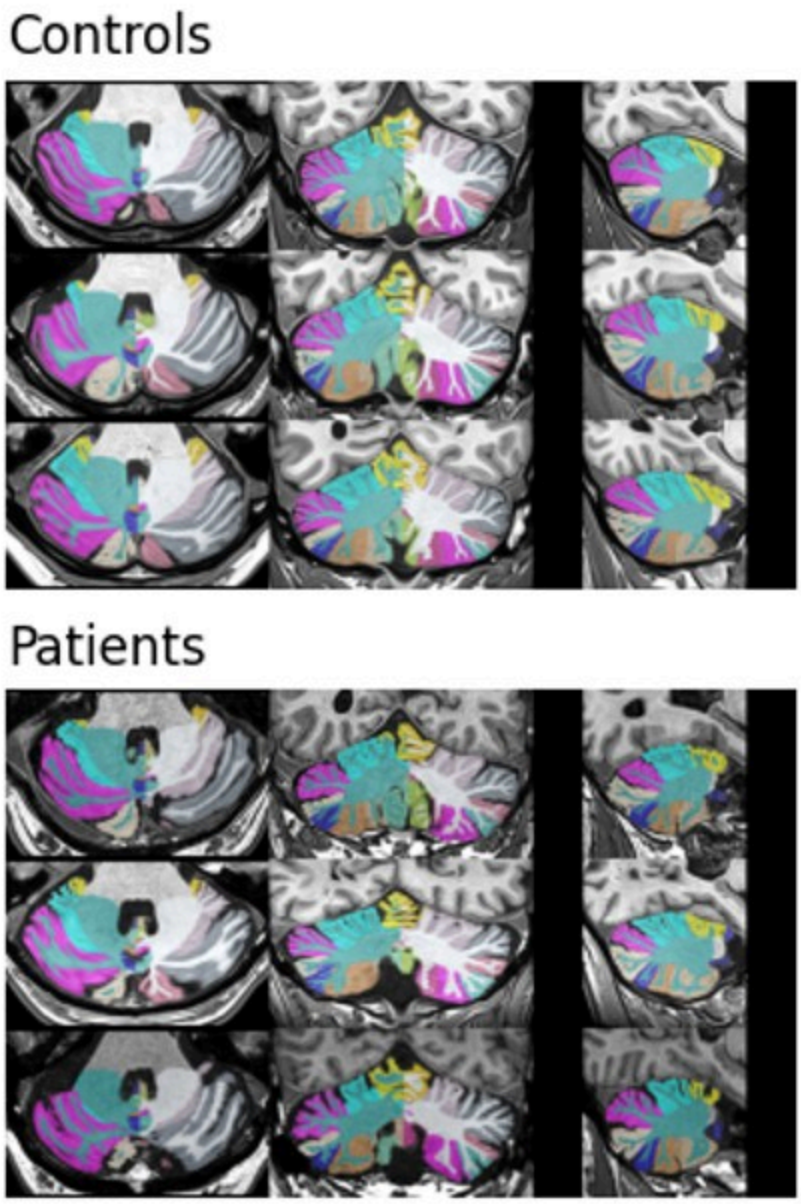


Figure 1

Examples of cerebellar segmentations obtained from the DeepCERES pipeline from three control subjects and three patients with SCA27B.

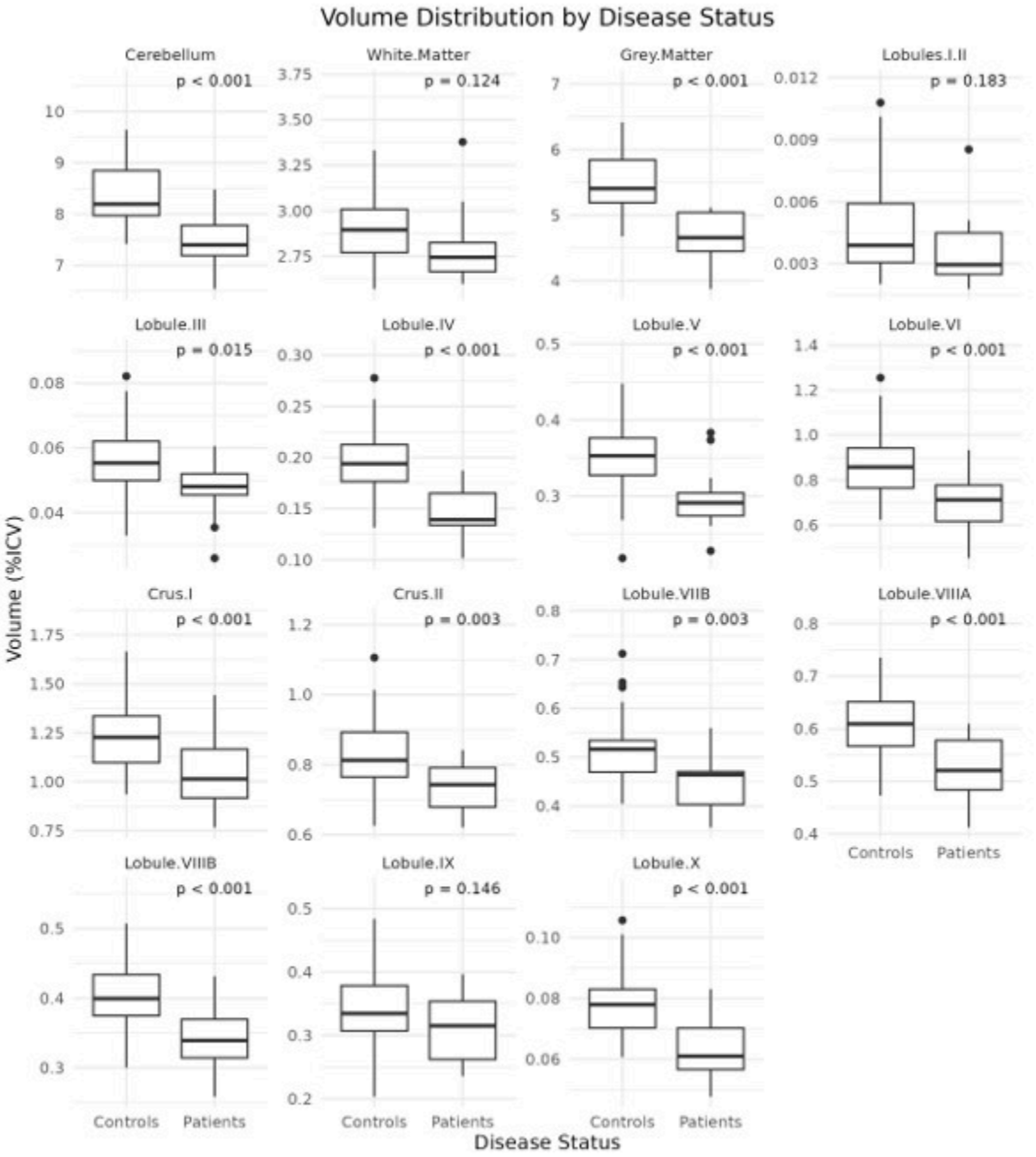


Figure 2

Boxplots for the volume (mean and interquartile range) of each region of interest calculated as percentage of intracranial volume (%ICV) for controls and patients with SCA27B. P values are obtained using ANCOVA and adjusted for false discovery rate.

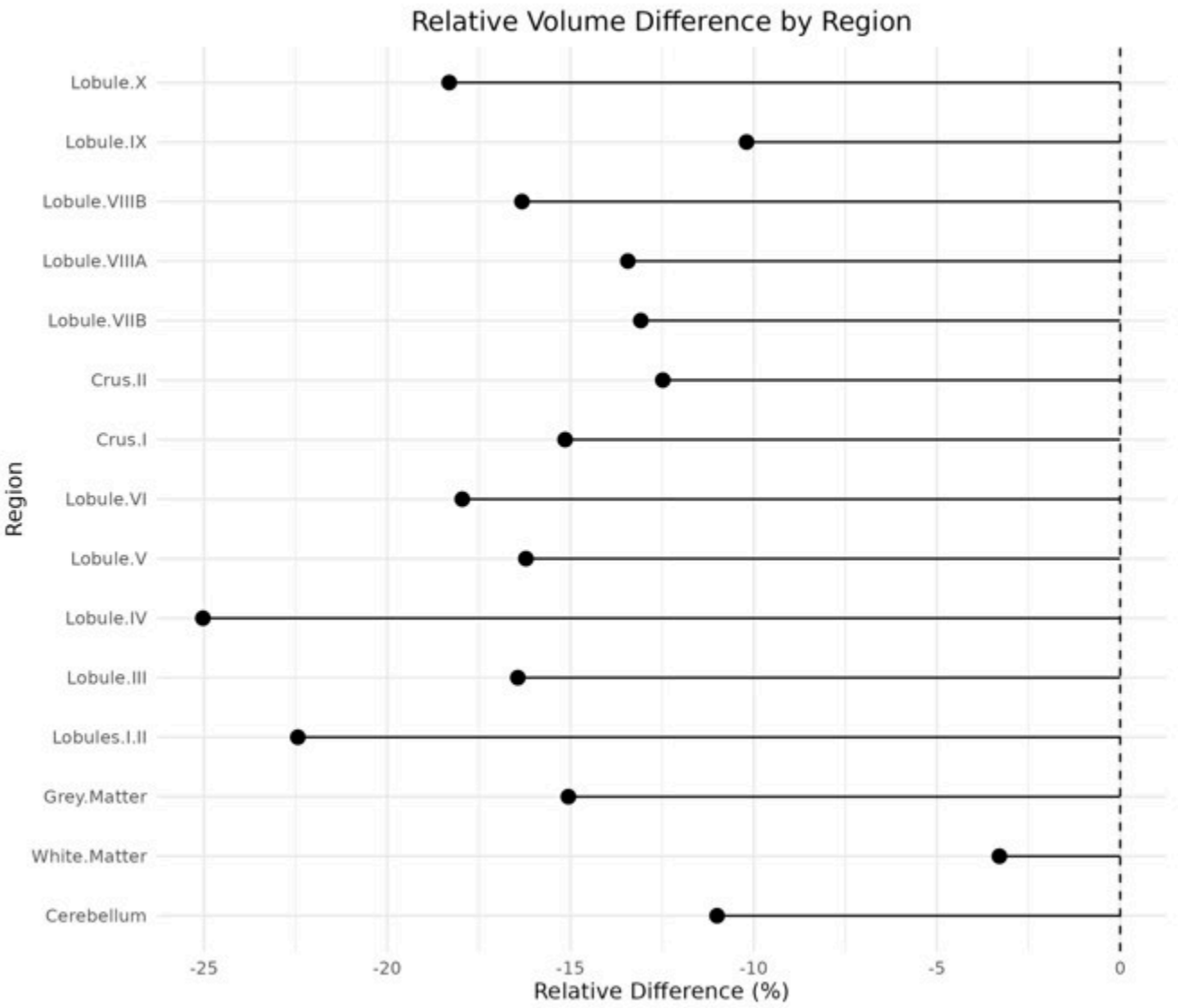


Figure 3

Relative volume difference expressed in percentage for each region of interest between patients with SCA27B and controls. Of note, the difference of volume between patients and controls was not statistically significant for the total white matter, lobules I-II and lobule IX (see also Table 1).

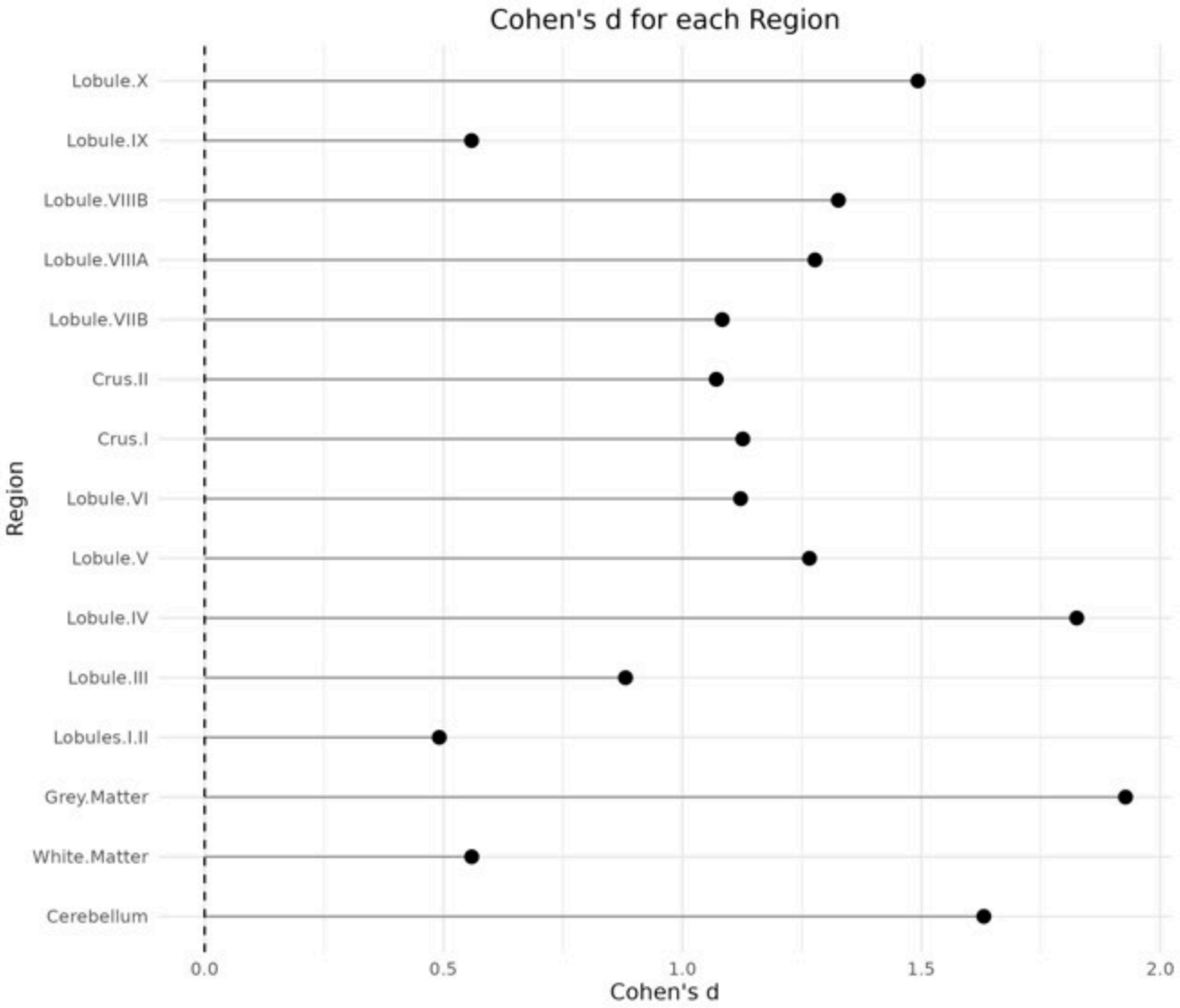


Figure 4

Effect of disease status on the volume of each region of interest presented with Cohen's d values. Cohen's values above 0.8 are classified as having large effect.